



HAL
open science

Emissions and transport of urban biocides from facades to topsoil at the district-scale

Laura Sereni, Tobias Junginger, Sylvain Payraudeau, Gwenael Imfeld

► **To cite this version:**

Laura Sereni, Tobias Junginger, Sylvain Payraudeau, Gwenael Imfeld. Emissions and transport of urban biocides from facades to topsoil at the district-scale. *Science of the Total Environment*, 2024, 954, pp.176269. 10.1016/j.scitotenv.2024.176269 . hal-04733852

HAL Id: hal-04733852

<https://hal.science/hal-04733852v1>

Submitted on 13 Oct 2024

HAL is a multi-disciplinary open access archive for the deposit and dissemination of scientific research documents, whether they are published or not. The documents may come from teaching and research institutions in France or abroad, or from public or private research centers.

L'archive ouverte pluridisciplinaire **HAL**, est destinée au dépôt et à la diffusion de documents scientifiques de niveau recherche, publiés ou non, émanant des établissements d'enseignement et de recherche français ou étrangers, des laboratoires publics ou privés.



Distributed under a Creative Commons Attribution 4.0 International License



Emissions and transport of urban biocides from facades to topsoil at the district-scale

Laura Sereni^{a,b,1}, Tobias Junginger^{a,c,1}, Sylvain Payraudeau^a, Gwenael Imfeld^{a,*}

^a Institut Terre et Environnement de Strasbourg (ITES), Université de Strasbourg/EOST/ENGEES, CNRS UMR 7063, F-67084 Strasbourg, France

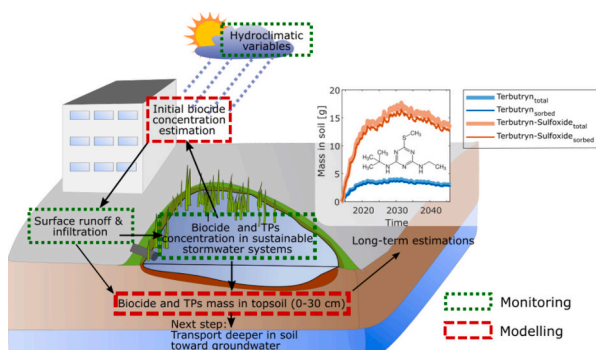
^b Université Grenoble Alpes, CNRS, INRAE, IRD, Grenoble INP, IGE, Grenoble, France

^c University of Stuttgart, Institute for Modelling Hydraulic and Environmental Systems (IWS), Research Facility for Subsurface Remediation (VEGAS), Pfaffenwaldring 61, 70597 Stuttgart, Germany

HIGHLIGHTS

- Biocides in building facades pose a chronic contamination risk at the district scale.
- Emission, storage, and leaching of the herbicide terbutryn were quantified.
- Terbutryn infiltrated into soil near facades and accumulated in topsoil.
- Terbutryn concentrations in runoff near facades exceeded PNEC values.
- The modeling approach enabled to quantify biocide fluxes at the district scale.

GRAPHICAL ABSTRACT



ARTICLE INFO

Editor: Jay Gan

Keywords:

Biocide fluxes
Sustainable stormwater system
District scale
Plant uptake
Leaching transport model
Triazine herbicide

ABSTRACT

Urban biocides used in facade paints and renders to prevent algae and fungal growth are released into the environment during rainfall, subsequently contaminating groundwater. However, quantitative data on the emission, transport and infiltration of urban biocides at the district scale are generally lacking. In this study, we quantified the fluxes of the urban biocide terbutryn and its major transformation product, terbutryn-sulfoxide, from building facades into stormwater, sediment, soil, and vegetation within a seven-year-old district employing sustainable stormwater management such as infiltration trenches and ponds. Combining four months of field observations with district scale modeling, we estimated initial concentrations of terbutryn in facade paint, quantified the emissions of terbutryn and terbutryn-sulfoxide from facades to soil, and evaluated terbutryn storage in soil under various painting scenarios. Terbutryn concentrations in sustainable stormwater management systems ranging from 2 to 67 ng L⁻¹, frequently exceeding predicted no-effect concentrations. The constant release of terbutryn and its transformation products in runoff highlighted the chronic exposure of non-target organisms to urban biocides. Terbutryn concentrations in topsoil and pond sediment indicated accumulation, while concentrations exceeding 1 μg g⁻¹ in the vegetation suggested plant uptake. Model results revealed that a substantial portion (27 to 73 %) of biocides infiltrated near facades through permeable surfaces like gravel, while

* Corresponding author.

E-mail address: imfeld@unistra.fr (G. Imfeld).

¹ These authors contributed equally to this work.

<https://doi.org/10.1016/j.scitotenv.2024.176269>

Received 22 July 2024; Received in revised form 6 September 2024; Accepted 12 September 2024

Available online 18 September 2024

0048-9697/© 2024 The Authors. Published by Elsevier B.V. This is an open access article under the CC BY license (<http://creativecommons.org/licenses/by/4.0/>).

a smaller portion (7 to 39 %) reached the stormwater management systems. Additionally, significant biocide leaching in the topsoil (30 cm below the surface) underscored the potential for biocide contamination in groundwater. Overall, this district-scale study and modeling approach provide a comprehensive framework for evaluating scenarios and measures for sustainable stormwater management to mitigate the infiltration of urban biocides into groundwater.

1. Introduction

Current urban planning incorporates sustainable stormwater management (SSM) strategies at the district scale to facilitate the direct infiltration of stormwater runoff through ditches and swale systems, directing it towards groundwater (Barbosa et al., 2012; Goulden et al., 2018). However, stormwater carrying urban contaminants, such as biocides, may infiltrate the soil, thereby posing a risk of groundwater contamination (Hensen et al., 2018; Linke et al., 2021; Vijayaraghavan et al., 2021). In urban settings, biocides are commonly added to building materials, such as facade paint and render, to prevent infestations by algae, mosses, fungi, and bacteria (Burkhardt et al., 2011; Pajjens et al., 2021). Biocides can leach from facades during rainfall events, leading to constant emissions over time (Hensen et al., 2018; Junginger et al., 2023; Linke et al., 2021; Pajjens et al., 2021; Vega-Garcia et al., 2020). In addition, the release of biocide transformation products (TPs) following photodegradation on the facades can exceed that of biocides (Bollmann et al., 2016, 2017b; Hensen et al., 2018; Junginger et al., 2023; Linke et al., 2021). Consequently, urban biocides and their TPs have been frequently detected in rivers, soil, and groundwater, with concentrations surpassing predicted no-effect concentrations (PNEC) (Burkhardt et al., 2011; Hensen et al., 2018; Linke et al., 2021, 2023; Pajjens et al., 2021; Quednow and Püttmann, 2007; Wittmer et al., 2010).

Knowledge of the distribution of biocides and their infiltration towards groundwater at the district scale is currently limited, which hinders the identification of measures to mitigate biocide emission, transport and groundwater contamination. This mainly arises from the scarcity of comprehensive datasets and modeling approaches at the district scale. Previous studies primarily focused on biocide release from freshly painted experimental facades (Junginger et al., 2023; Vega-Garcia et al., 2020), and their subsequent infiltration through stormwater management systems, including biocide leaching from soil into groundwater (Hensen et al., 2018; Pinasseau et al., 2020). The preferential infiltration of biocides through soil macropores may significantly contribute to biocide leaching into groundwater (Bork et al., 2021). However, comprehensive district-scale quantitative estimations of biocide transport are particularly lacking, including long-term (>1 year) emissions from facades, hotspots of biocide degradation and accumulation, and preferential pathways of biocide infiltration to groundwater.

To estimate long-term biocide emissions from facades, various models, including COMLEAM (Construction Material Leaching Model) and FReWaB-PLUS (Freiburger Regenwasser-Bewirtschaftung – Plus Stofftransport), have been developed (Bork et al., 2022; Burkhardt et al., 2020; Coutu et al., 2012a; Wittmer et al., 2011). These models integrate material properties, building geometry, and weather data, encompassing variables such as rainfall, wind speed, and wind direction, to infer wind-driven rain as the primary factor driving biocide emission. However, substantial variations exist among the models concerning the spatial and temporal resolutions of biocide emission. Additionally, the models ability to quantify biocide emission and transport is constrained by the heterogeneity of the district catchment, including land-use, permeable surface-soil interfaces, the age and orientation of facades, and prevailing hydro-climatic conditions. As a result, current models do not account for the release and transport of biocide TPs from facades (Burkhardt et al., 2020; Coutu et al., 2012a) despite evidence of biocide transformation on the facades (Bollmann et al., 2016; Junginger et al., 2023). Overall, comprehensive modelling approaches of biocide

emission, infiltration and leaching into soil and groundwater at the district scale are mostly lacking. This hinders the identification of management scenarios to protect water quality within SSM schemes, while also addressing ecotoxicological risks.

The aim of this study was thus to quantify biocide emission, transport, and storage at the district scale, focusing on the associated ecotoxicological risks and biocide infiltration into soil within the context of SSM. Terbutryn, a commonly used herbicide in paints, was selected as a model urban biocide due to its widespread use in facade paints and renders, its ubiquitous detection in urban areas (Bollmann et al., 2017a; Hensen et al., 2018; Quednow and Püttmann, 2007), and its known toxicity (Burkhardt et al., 2009; Kresmann et al., 2018). The field campaign involved a four-month monitoring of hydroclimatic parameters, water runoff, and terbutryn and its transformation products (TPs) in water, soil, sediment, and plants within a 2.4-hectare district (Schiltigheim, Strasbourg, France) designed with an SSM scheme. These field observations were complemented by a modeling approach to estimate the initial concentration of terbutryn in building paint, evaluate terbutryn emissions in runoff from building facades, and assess soil infiltration towards groundwater, as well as storage and degradation at the district scale. The modeling examined the effects of various facade painting scenarios, with and without terbutryn, on the accumulation of terbutryn and its primary transformation product, terbutryn-sulfoxide, in soil over 30 years.

2. Material and methods

2.1. Study site

The study area, covering 1.24 ha within a 2.4 ha district, is located in Schiltigheim in the northern part of Strasbourg, France (coordinates: 48°36'31.7"N, 7°44'54.8"E; Fig. 1). Constructed in 2014, the district includes two sub-catchments, with water drainage directed either towards a vegetated stormwater infiltration pond or an infiltration trench (Figs. S1 and S2). The infiltration zone was designed to channel the district rainwater into the subsurface. The underlying soil primarily consists of sandy loess, with a hydraulic conductivity of 10^{-4} m s⁻¹. In the pond, a small area remains permanently flooded. However, during periods of elevated water levels, water can infiltrate through a designated infiltration area. During heavy storm events, excess water is directed into infiltration wells surrounding the pond. These wells bypass the loess layer and infiltrate water directly into a sand and gravel layer at a depth of 4 m.

The trench functioned similarly to a swale system, facilitating water infiltration into the soil. Under normal conditions, it allowed water to infiltrate by gravity through the vegetated surface, which has a hydraulic conductivity of 10^{-4} m s⁻¹. However, during heavy rainfall, the low permeability of the loess soil may cause water levels to rise. Therefore, an overflow system was installed to divert excess water to the infiltration basin.

The district comprises ten buildings and a playground area. Field sampling and monitoring were conducted between May 5th and August 24th, 2021. During this period, the wind, which was the driving force behind wind-driven rain, predominantly came from the south.

The land use and sub-catchments that discharge either into the trench or pond system were identified by field survey with a specific focus on the ground-facade interface and from LIDAR (Light Detection and Ranging) data, respectively (Figs. 1, S1–S2 and Table S1). The land

use categories of areas directly adjacent to facades included lawn, impermeable pavement, gravel, concrete pathways, and wood chips. For areas not directly adjacent to facades, land use categories included concrete pathways, paving with narrow spacers, irregular stone paving, and various permeable surface-soil interfaces such as lawn, gravel, and playground areas (Fig. 1). Empirical runoff coefficients were obtained from the FRWaB-PLUS database (Bork et al., 2022) (Table S1b and Fig. 1).

Building attributes, including height and surface area, were extracted from LIDAR data and analyzed within a GIS (Fig. S3) to estimate facade areas. The proportion of windows, determined through on-site photographs and field surveys, was considered to contribute to facade runoff but not to biocide leaching. Windows represented 23.5 % and 25.3 % of the building surfaces for pond and trench catchments, respectively.

Continuous monitoring of runoff at the outlets of the sub-catchments, specifically the trench and pond inlets (Fig. 1), was conducted using a flowmeter (ISMA DLK 102) with a 1 min resolution. This flowmeter was connected to a venturi channel equipped with an ultrasonic sensor. The water level within the pond was monitored using a CTD diver (DI 282) with a 5 min resolution, incorporating barometric compensation (Baro-Diver DI 800). Elevation-storage curves for the trench and pond were derived from water level and LIDAR data.

2.2. Sampling

Water sampling was conducted using an automated sampler (ISCO Avalanche) with 12 bottles (330 mL). The sampler was connected to the

flowmeter to enable discharge-proportional sampling. A sampling strategy was devised to cover both minor and major runoff events. For the first 9 bottles, 110 mL of water was collected for every 1 m^3 of runoff, distributed over three consecutive increments into the same bottle. Subsequently, 110 mL was collected after every 10 m^3 of runoff, again in three separate increments, until all 12 bottles were filled. The recorded water level dynamics and elevation-storage curves were employed to reconstruct runoff dynamics during major events on June 22nd and July 15th, when venturi channels were flooded, hindering accurate runoff measurement and automated sampling.

Grab water samples were collected weekly or bi-weekly from both the trench and the pond, except when water levels dropped below 5 cm, preventing sampling. These samples, totaling 5 L for the trench and 10 L for the pond, were collected by taking 5 subsamples using a cleaned telescopic scoop, which were then combined into a single composite sample. All water samples underwent sequential filtration at $11 \mu\text{m}$ (Whatman 1001-047) and $0.45 \mu\text{m}$ (CA membrane filter) and were stored at $4 \text{ }^\circ\text{C}$ for $<24 \text{ h}$ until further analysis.

Soil and sediment samples were collected monthly from May 4th to July 27th, 2021. Subsamples were collected from the uppermost 10 cm within a $50 \times 50 \text{ cm}$ area. To maintain consistency, surface materials such as grass, roots, and debris within the top 5 cm were removed using a cleaned shovel. The shovel was thoroughly cleaned, starting with the removal of large particles and debris. It was then washed with demineralised water, scrubbed with a stiff brush, and followed by another rinse with demineralised water. In the trench, five soil subsamples were collected at 1 m intervals across a 5 m span from the main inlet and combined to create a single composite sample. In the pond, five

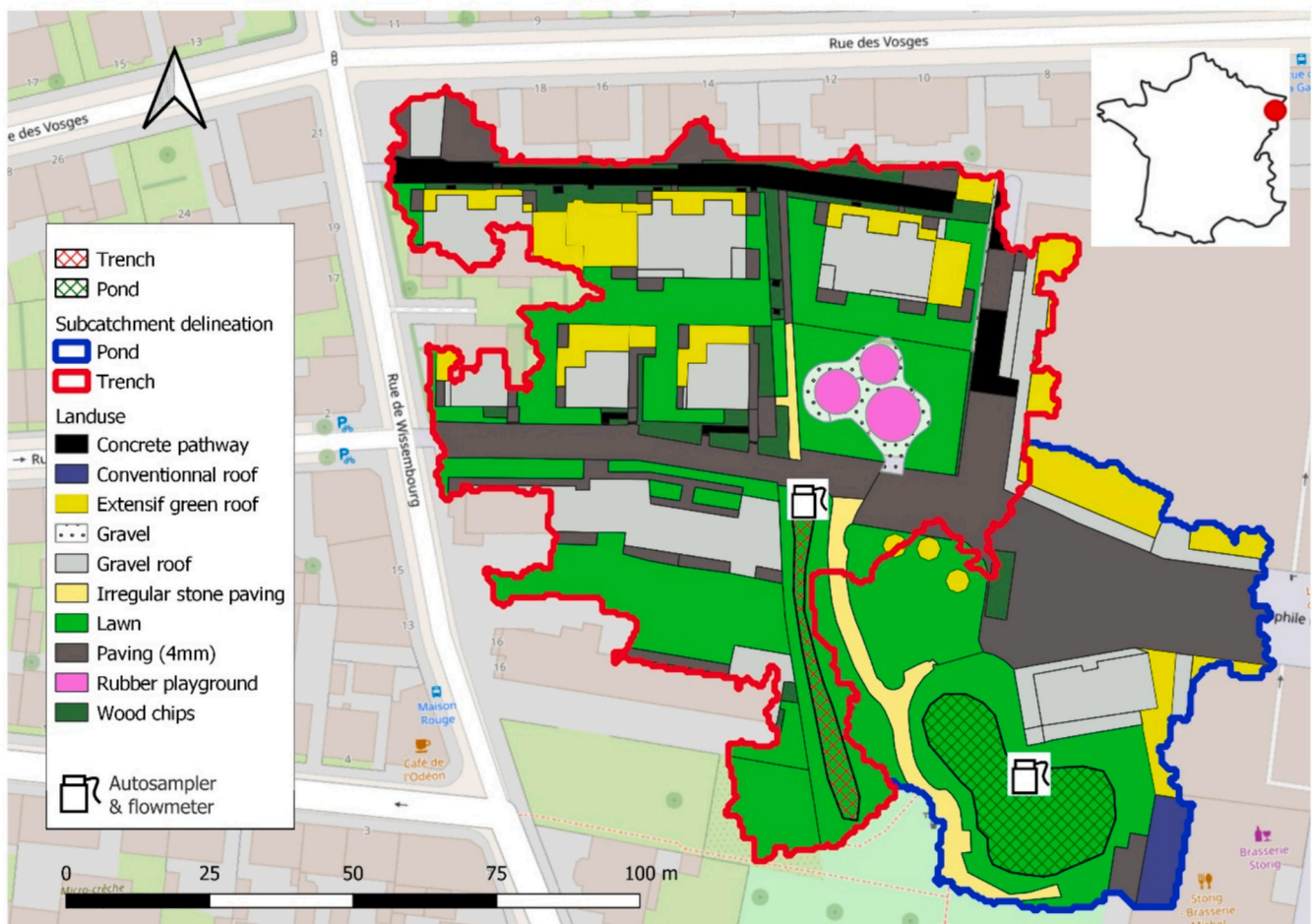


Fig. 1. Landuse and sustainable stormwater management systems of the Adelshoffen district (Schiltigheim, France).

sediment samples were taken from various locations and analyzed individually. The samples were stored at 4 °C and biocide extracted within 24 h (see Section 2.3). Physico-chemical characteristics of the mixed composite soil and sediment samples (Table S2) were measured using standard analytical procedures (Table S2).

In the infiltration pond, specimens of *Phragmites* sp. (Cav.), covering 60–80 % of the pond surface, were collected from five randomly selected locations. Five grass samples were collected from the trench, with one sample taken at each meter interval across a 5 m stretch starting from the inlet. The five plant samples were divided into their aerial and root parts, which were combined separately into one composite sample. All collected samples were transported to the laboratory within 2 h. The roots were washed in ultrapure water for 10 min, with the water replaced until turbidity remained constant. They were then rinsed twice with a 0.9 % NaCl solution (ACS reagent, ≥99.0 % in ultrapure water) to eliminate sediment (Gilevska et al., 2022). The samples were then homogenized using a blender (Bosch MSM66110) and frozen at −20 °C until biocide extraction.

2.3. Biocide extraction and analysis

Biocides in sediment, soil and plant samples were extracted in triplicates using a ultrasonic-assisted solid-liquid extraction protocol (Gilevska et al., 2022), detailed in SI. Briefly, 5 g of soil or sediment (dry weight) and 3 g of plant material were placed in an amber glass centrifuge tube. Samples were extracted using 3 mL DCM: Pentane (3:1, v:v), followed by vortexing (5 s) and ultrasonication (5 min). The solvents were separated from the sample by centrifugation at 2400 rpm for 20 min. Supernatants were transferred to amber glass vials, and the procedure was repeated two more times. The solvents were evaporated under a N₂ stream and resuspended in 1 mL of acetonitrile. All samples were cleaned before measurement using anhydrous magnesium sulfate (MgSO₄, 75 mg) and primary-secondary amine (PSA bond silica, 13 mg).

Terbutryn, four of its TPs (terbutryn-sulfoxide, terbutryn-2-hydroxy, terbutryn-desethyl, terbutryn-desethyl-2-hydroxy), diuron and octylisothiazolinone were quantified using HPLC-MS/MS (Dionex/Thermo Scientific UltiMate Dionex 3000 coupled to Thermo Scientific TSQ Quantiva), with LOQ < 4.5 ng L⁻¹ (Junginger, 2023; Junginger et al., 2022). Instrument settings and recovery rates are provided in Table S3.

2.4. Hydrological balance at the district scale

A hydrological balance for the trench and pond sub-catchments was established by considering rainfall, direct infiltration at the base of building facades, diffuse infiltration across buildings, and runoff from ground-facade and surface-soil interfaces (Fig. 1). Infiltration and evaporation were also estimated for the trench and the pond as key elements of the SSM in this district. Combined with biocide concentration data, this enabled the quantification of biocide emission and transport under different painting scenarios. The campaign targeted two distinct periods: from May 5th to May 31st, 2021, referred to as the ‘spring period’, and from June 20th to August 5th, 2021, denoted as the ‘summer period’ (Fig. S4). Precipitation was recorded with a local weather station (DAVIS Vantage Vue 6020) located at the field site, with measurements taken at a 10 min resolution.

Rainfall and runoff events for the spring and summer periods were defined by a minimum of 20 h without precipitation. Rainfall intensity and depth were evaluated using the IETD R package (Duque, 2020). The rainfall volume for each event was calculated for the trench and pond sub-catchments, considering their respective areas.

For each rainfall event, the cumulative runoff volume entering both the trench and the pond, along with the corresponding diffuse runoff coefficient, were computed using the flowmeter dataset. During intense runoff events, when the venturi channel and flowmeter were flooded, the runoff volume entering the pond was reconstructed using water level sensors and the surface-elevation-storage curve. The filling-emptying

dynamics in the trench and pond were corrected by accounting for evaporation from the submerged surfaces and infiltration. The daily potential evapotranspiration (PET) was provided by MeteoFrance (Entzheim, located 11.5 km southeast of the district at 48.55°N, 7.63°E). Pond and trench infiltration rates were estimated from recorded water levels and elevation-storage curves using linear and exponential models (R lm and nls regression functions). These calibrated infiltration rates, derived from observed filling-emptying dynamics, were consistent with values provided in the SSM technical report of the district, which were based on in situ soil infiltration tests.

2.5. Biocide long terms release and transport under painting scenarios

A model was developed to examine the long-term biocide release and transport from facades to urban topsoils under two contrasting painting scenarios. Both modeling scenarios involve repainting in 2024, a decade after the construction of the district in 2014, following the manufacturer's recommendations. In scenario P1, facades were repainted with the same type of paint used in 2014, containing the same amount of terbutryn. Under this scenario, biocide emissions during the 2024–2034 period are similar to those of the 2014–2024 period, leading to continued accumulation in soils and water. In scenario P2, facades were repainted with biocide-free paint, covering the previous layers and resulting in zero biocide emissions from the facades. In this case, biocide emissions only occurred during the 2014–2024 period. Therefore, it is important to assess the degradation and retention time of biocides in soil once emissions cease. Model calculations were extended until 2045 to examine the release and persistence of biocides in topsoil. We hypothesized that all facades were painted in the same manner and with the same paint, given that the entire district was built at the same time.

In brief, we built upon an existing biocide leaching model (COMLEAM, (Burkhardt et al., 2020)) that provides mathematical formulations for biocides leaching. Facade leaching experiments conducted by our team were used to calibrate the model (Junginger et al., 2023). The leaching model was further supplemented by transport, infiltration, and reaction processes. Infiltration coefficient were extracted from the database of FRWaB-PLUS (Bork et al., 2022). Additionally, degradation rates of terbutryn and terbutryn-sulfoxide were incorporated based on laboratory and outdoor experiments (Junginger, 2023; Junginger et al., 2022). Hence, the biocide emission and transport model comprises the following components: (i) terbutryn transformation on facades into its major transformation product, terbutryn-sulfoxide, depending on solar irradiation since the last rain event (Junginger et al., 2023); (ii) terbutryn leaching from facades, using a modified version of COMLEAM (Burkhardt et al., 2020), with parameters tailored from field surveys, accounting for leaching of both terbutryn and terbutryn-sulfoxide; (iii) direct infiltration and runoff at the ground-facade interface, diffuse runoff and infiltration occurring during transport into stormwater management systems, and direct pond and trench infiltration; and (iv) first-order kinetics for terbutryn degradation into terbutryn-sulfoxide, as well as the further degradation of terbutryn-sulfoxide into secondary transformation products in the topsoil.

Biocide emission from facades was modeled at an hourly resolution (SI, Section 1.4) following the COMLEAM guidelines, while biocide transport, degradation, and sorption were computed at a daily resolution. Since no information on initial terbutryn (C₀) concentrations on building facades was available at the district scale, a back calculation of C₀ was performed using the model, starting from 2014 and utilizing concentration data of biocide in runoff collected in 2021.

The predicted masses of biocides and TPs infiltration into topsoil ($M_{Infiltration_{biocide+TP}}$) and those reaching the SSM systems, i.e., trench or pond outlets ($M_{Outlet_{biocide+TP}}$) in each sub-catchment (SC) were calculated with Eqs. (1) and (2), respectively. These calculations were based on the diffuse runoff coefficient for the sub-catchment (RC_{DIFF, SC}) calculated from the 2021 campaign, the direct runoff coefficient (RC_{DIRECT, SC}) according to ground-facade types, the FRWaB-PLUS database, and the

emitted mass of biocide and TP from facades ($E_{biocide+TP}$):

$$M.Inf_{biocide+TP}(SC, t) = (1 - RC_{DIRECT,SC}) \times (1 - RC_{DIFF,SC}) \times E_{biocide+TP}(SC, t) \quad (1)$$

$$M.Outlet_{biocide+TP}(SC, t) = RC_{DIRECT,SC} \times RC_{DIFF,SC} \times E_{biocide+TP}(SC, t) \quad (2)$$

The topsoil biodegradation half-lives (DT_{50}) for terbutryn were derived from outdoor lysimeter experiments conducted in 2021 within the district under similar climatic conditions and for typical top surfaces of SSM districts. The DT_{50} values for sand, gravel, and soil were 68, 64, and 61 days, respectively (Table S1c), based on previous leaching experiments described in Junginger et al. (2023). Similar DT_{50} values were obtained for terbutryn-sulfoxide according to the lysimeter experiments. Partitioning between sorbed and dissolved phases in topsoil was estimated using the partitioning coefficients (K_D) derived from the organic carbon-water partitioning coefficients (K_{OC}) (European Commission, 2011) and the organic carbon content (OC) specific to various surface-soil interfaces (Table S1b). In the absence of specific references, the K_{OC} values for terbutryn were used for terbutryn-sulfoxide. At each daily time step, a linear sorption equilibrium in the soil was assumed, considering both freshly infiltrated terbutryn and terbutryn-sulfoxide alongside the pre-existing stock. Only the dissolved fraction of terbutryn and terbutryn-sulfoxide was considered available for degradation.

Additional climatic data was collected to simulate biocide emission and persistence from 2014 to 2045. Hourly rainfall and daily evaporation, wind speed, and global irradiation data from 2014 to 2021 were duplicated to cover a 30-year period (2014–2045), assuming steady climate conditions across scenarios. Hourly rainfall from 2014 to 2021 was calculated as the mean value of the two closest rain gauges (Schiltigheim gauge, 5 km southeast, and Bischeim gauge, 5 km northwest). Daily data on evaporation, wind speed and direction, and global irradiation were obtained from the MeteoFrance weather station in Entzheim for the period 2014 to 2021. These data were used to calculate wind-driven rain, which is more reliable than vertical rain for predicting biocide leaching in the leaching model (Bester et al., 2014; Bollmann et al., 2014). Global irradiation data for each azimuth was obtained from the EU photovoltaic GIS (European Commission, 2022). This data was used to generalize equations relating irradiation and biocide release, initially derived for experimental facades oriented only to the West (Junginger et al., 2023 and Fig. S5).

The COMLEAM leaching model was originally developed for application to a limited subset of buildings, considering each segment of facade as a unit characterized by uniform height, window proportion, and orientation (i.e., N, NW, W, SW, S, SE, E, and NE). However, given the significant number of facade segments at the district scale (i.e., 323 in Adelshoffen district) and associated computation time, facade portions were aggregated based on their orientation, associated sub-catchment (i.e., connected to trench or pond), and combination of facade-ground-land use interfaces. This aggregation resulted in 11 segments used to calculate direct and diffuse infiltration and runoff fluxes. Diffuse infiltration and runoff between the ground-facade interface and SSM were calculated for each land use and averaged per sub-catchment (Table S1c). Equations and data processing steps are provided in the SI (Section 1.4).

3. Results

3.1. Hydrological balance at the district scale

In 2021, recorded rainfall was 109 mm in spring and 299 mm in summer, contributing to a total annual rainfall of 929 mm. The event-based runoff coefficients showed little variation, with the trench having a coefficient of $39 \pm 7\%$ and the pond $36 \pm 4\%$ for moderate intensity events ($<200 \text{ m}^3$ precipitation/event; $n = 11$ events for the trench, and $n = 31$ for the pond). For the trench sub-catchment, the

cumulative runoff volume represented 40 % of the total rainfall volume in spring and 30 % of the rainfall volume in summer (Fig. S8 and S9a). For the pond sub-catchment, the cumulative runoff volume during the spring and summer periods (Fig. S9b) corresponded to 40 % and 90 % of the rainfall, respectively, with three storm events generating more intense runoff in the pond than in the trench sub-catchment. Empirical runoff coefficients (Table S1b) derived from the land-use map and FReWaB-PLUS database were 44 % and 49 % for the trench and pond sub-catchments, respectively (Table S1c), showing $<5\%$ deviation compared to observed runoff coefficients. Wind directions and speeds are provided in Fig. S6 (SI). On a seasonal scale, direct evaporation from the trench and pond was 20 to 50 times smaller than the rainfall volume (Fig. S7).

In both sub-catchments, only a minor portion of runoff from facades, and consequently, the emitted biocides, eventually reached the trench or the pond. Direct infiltration at ground-facade interfaces accounted for 73 % in the trench sub-catchment and 31 % in the pond sub-catchment (Table S1c). For the remaining water from direct runoff, diffuse infiltration between the base of facades and SSM ranged from 60 % to 70 % in the trench sub-catchment and from 10 % to 65 % in the pond sub-catchment, considering minimal and maximal runoff coefficients. Hence, at the district scale, 72 % to 86 % of direct rainfall volume and facade runoff infiltrated into the soil, while the remaining volume fraction entered into the SSM.

3.2. Biocides concentration in pond and trench

Terbutryn was consistently detected in soil, sediment, and plants in 2021 (Fig. 2). Weekly grab samples of water from the infiltration trench revealed concentrations of terbutryn and its four TPs higher than those observed in the pond (Fig. 2a). Additionally, concentrations of terbutryn TPs in the trench frequently surpassed those of terbutryn itself. The consistent detection of terbutryn and its TPs seven years after the district construction aligns with previous studies, highlighting the continuous release of terbutryn and its TPs from facades over time due to wind-driven rain (Hensen et al., 2018; Linke et al., 2021; Wicke et al., 2022). High concentrations for terbutryn-sulfoxide, identified as a major terbutryn TP formed during photodegradation on facades and biodegradation (Bollmann et al., 2016, 2017a; Junginger et al., 2022), were predominantly observed in the trench. This finding aligns with previous field studies (Bollmann et al., 2016; Burkhardt et al., 2011; Hensen et al., 2018; Linke et al., 2021).

In contrast to terbutryn, diuron concentrations in the trench were consistently lower than those in the pond but still exceeded 100 ng L^{-1} (Fig. 2b). Notably, OIT was not detected in either SSM system. The variable concentrations of terbutryn and diuron in the pond and trench suggest that different types of paints, each containing distinct proportions of terbutryn and diuron, were used in these sub-catchments. However, differences in the initial concentrations of biocides among the buildings cannot be ruled out.

In both the trench and the pond, runoff concentrations regularly exceeded the PNEC values for terbutryn (ranging from 3 to 34 ng L^{-1}) and diuron (20 ng L^{-1}) (Burkhardt et al., 2009; Kresmann et al., 2018). Therefore, even seven years after the construction of the district, ecotoxicological risks associated with biocides existed, especially considering the chronic exposure of soil and aquatic organisms (Reiß et al., 2024). However, there is a lack of sufficient ecotoxicological data related to the effect of urban biocides on the soil as well as surface water and sediment microbiomes (Reiß et al., 2021). Additionally, the cumulative inhibition of bacterial growth observed over time in the case of terbutryn (Fernández-Calviño et al., 2021) suggests that chronic exposure to biocide, such as ongoing facade runoff during each rainfall event, may be underestimated.

Soil and sediment samples provided evidence of terbutryn retention during infiltration processes. Terbutryn accumulated notably in the trench soil (Fig. 2c), with concentrations exceeding $1.5 \mu\text{g kg}^{-1}$, whereas

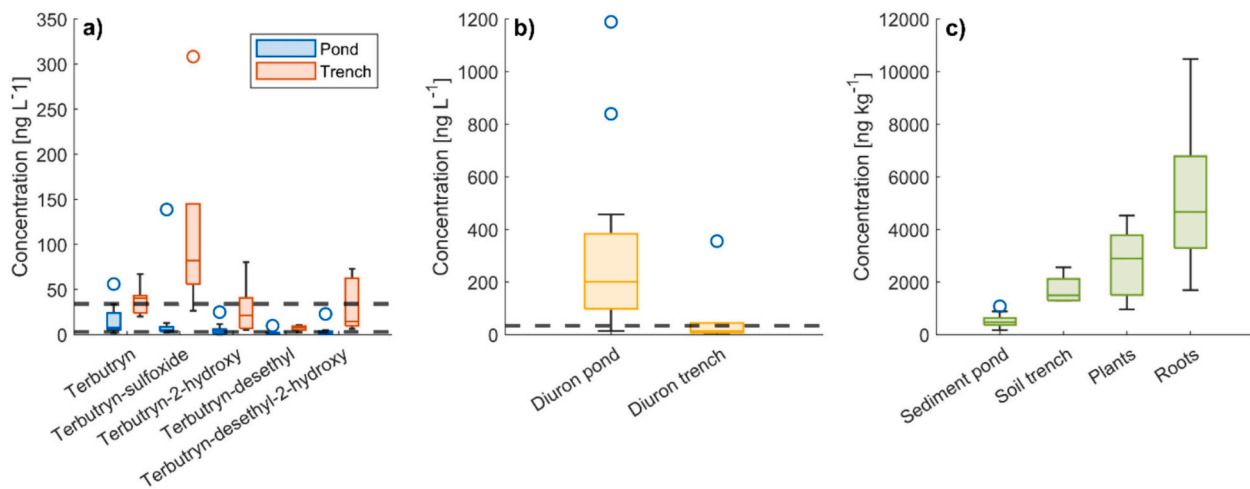


Fig. 2. Concentrations of (a) terbutryn and its transformation products in the pond ($n = 13$) and trench ($n = 6$), (b) diuron in the pond ($n = 13$) and trench ($n = 6$), and (c) terbutryn in sediment ($n = 20$), soil ($n = 4$), and plants and roots (ng kg^{-1} dry weight). Dashed lines indicate PNEC values for terbutryn (ranging from 3 to 34 ng L^{-1}) and diuron (20 ng L^{-1}). Circles represent outliers, identified as data points that are >1.5 times the interquartile range from the top or bottom of the box.

concentrations in pond sediment reached $0.5 \mu\text{g kg}^{-1}$. The higher concentrations of terbutryn in the trench soil can be attributed primarily to greater terbutryn emissions within the trench sub-catchment, as observed in runoff (Fig. 2a). Additionally, the higher organic carbon content in trench soil compared to pond sediment (Table S2) may lead to higher sorption and thus more accumulation of terbutryn in the trench. Considering high sorption capacity ($\log K_{\text{OW}} = 3.43$; Finizio et al., 1991) and moderate persistence ($\text{DT}_{50, \text{soil}} \approx 60$ days) of terbutryn, both sediment and soil can mitigate terbutryn transport towards groundwater. Conversely, diuron was not detected in pond sediment and trench soil despite although it was quantified in runoff (Fig. 2a) and persisted in soil ($\text{DT}_{50, \text{soil}} = 29$ days, Junginger, 2023). This aligns with the higher mobility of diuron in soil ($\log K_{\text{OW}} = 2.45$; Finizio et al., 1997) and potential transport towards groundwater. Altogether, these results highlight contrasting accumulation patterns of terbutryn and diuron in topsoil, depending on their propensity to sorb and dissipate. The accumulation of biocides and their transformation products in soil and sediment carries the risk of chronic ecotoxicological effects, which may be heightened by additive or synergistic interactions resulting from the co-occurrence of biocides (Reiß et al., 2024).

Terbutryn was also detected in plant and root samples within the trench and pond systems, with concentrations exceeding $1 \mu\text{g kg}^{-1}$ (Fig. 2c). This confirms the occurrence of plant uptake, a phenomenon not previously reported for biocides in urban environments. Plant uptake of biocides could potentially serve as a significant sink for these substances in urban areas. It is possible that plants passively uptake and eventually metabolize urban biocides, thereby mitigating their transport towards groundwater. For instance, the uptake of terbutryn has been documented in parrot feather (*Myriophyllum aquaticum*) (Gao et al., 2000; Turgut, 2005). Similarly, the uptake and metabolization of isothiazolinones by hydroponically grown *Arabidopsis* was observed (Muerdter et al., 2022). Aquatic plants may thus contribute to phytoremediation strategies for various biocides. A more comprehensive understanding of plant uptake rates and the overall mass flux into plants at the district scale, as well as its seasonal variation, necessitates further investigation.

Using the volume of the pond, calculated from the storage-elevation curves, the mass of compounds in the water can be determined based on the measured concentrations. In general, the retained mass of terbutryn and its TPs in both the trench and pond water consistently remained below 1 mg for each compound. However, during a heavy rainfall event, the stored masses in the pond water increased significantly, reaching up to 8 mg for terbutryn, 42 mg for terbutryn-sulfoxide, 8 mg for terbutryn-2-hydroxy, 3 mg for terbutryn-desethyl, and 7 mg for terbutryn-

desethyl-2-hydroxy. This corresponded to emitted masses of $2 \mu\text{g m}^{-2}$ of facade for terbutryn and 10, 2, 3, and 1 $\mu\text{g m}^{-2}$ for terbutryn-sulfoxide, terbutryn-2-hydroxy, terbutryn-desethyl, and terbutryn-desethyl-2-hydroxy, respectively, on July 13th. These release rates are lower than those reported in other studies, which often exceed $100 \mu\text{g m}^{-2}$ per rain event (e.g., Bollmann et al., 2016; Junginger et al., 2023). Given the advanced age of the facades at our field site compared to the freshly painted facades in the literature, and considering that only a portion of the facades was likely exposed to weathering due to prevailing wind directions, our results are consistent with the values reported in the literature. Similar patterns were observed for diuron, with stored masses generally below 20 mg but increasing up to 250 mg during the same heavy rainfall event. This corresponded to an emitted mass of $61.4 \mu\text{g m}^{-2}$ for the entire district catchment. Consequently, although intense rainfall events were not consistently associated with elevated biocide concentrations due to dilution, they can lead to significant mass fluxes due to constant biocide emission from facades. Intense rainfall events may induce rapid direct infiltration or through infiltration wells around the pond bypassing filtering soil layers, transporting significant biocide loads towards groundwater. The biocide loads transported via infiltration wells were estimated at 150 and 530 μg of terbutryn, and 13 and 10 mg of diuron, for the events on May 18, 2021, and August 24, 2021, respectively.

Overall, the field campaign enabled the identification of prevailing biocide pathways from facades to groundwater at the district scale. However, deriving a comprehensive biocide mass balance was not achievable solely from observed data in accessible compartments, i.e., runoff, SSM systems, and topsoils. A modeling approach was thus developed and deployed at the district scale to estimate emissions since the district construction and to explicitly evaluate the reactive transport of biocides from facade to topsoil.

3.3. Biocide emissions and ecotoxicological risks on the district scale

The emission and transport model used observed biocide concentration data in runoff to estimate the initial concentration (C_0) of terbutryn on facades following painting in 2014. C_0 was back-calculated assuming that all the buildings were painted with paints containing terbutryn, as confirmed by local stakeholders. The occurrence of diuron in runoff suggested that other biocides were used in paints and renders at the district scale. The initial COMLEAM emission equations were modified using data from a previous outdoor facade experiment (Junginger et al., 2023). Considering data uncertainty, the terbutryn C_0 varied from 24 mg m^{-2} (low C_0) to 82 mg m^{-2} (high C_0).

Previously reported total terbutryn concentrations in paints were notably higher, spanning from 250 to 4000 mg m⁻² (Burkhardt et al., 2011; Coutu et al., 2012b; Schoknecht et al., 2016). This suggests that either paints with lower terbutryn concentrations were used in the district, or some facades were painted without terbutryn. The consistency in estimated C₀ values based on terbutryn, terbutryn-sulfoxide, and their sum (terbutryn + terbutryn-sulfoxide) underscored the robustness of the ratio between terbutryn and terbutryn-sulfoxide in the biocide emission model for C₀ estimation (Fig. S13).

In 2015, one year after district construction, the predicted cumulative emissions of terbutryn and terbutryn-sulfoxide from facades at the district scale ranged from 4.4 to 15.7 g, equivalent to 0.4 to 1.5 mg m² of facade (Fig. 3). Terbutryn contributed only 24 % of the total emissions, while terbutryn-sulfoxide accounted for the remaining 76 %. Terbutryn and terbutryn-sulfoxide emissions exhibited a slight decline over time, resulting in total emissions on the district scale ranging from 43.3 to 146.0 g (i.e., 4.1 to 14.0 mg m²) after 10 years.

At the ground-facade interface, predicted concentrations of terbutryn in runoff for each rainfall event were several orders of magnitude higher than the PNEC values and the annual average environmental quality standards (AAEQS) of 0.065 µg L⁻¹ (Whitehouse et al., 2011) (Fig. 4). Considering the upper limit of the initial terbutryn concentration (C₀) estimate, terbutryn concentrations in runoff entering the SSM exceeded PNEC values for 59 % of the events, while the AAEQS was surpassed in 12 % of the events. Currently, there is a scarcity of ecotoxicological studies and data available for terbutryn TPs, limiting risk estimations (Luft et al., 2014). Nevertheless, terbutryn TPs may exhibit similar toxic effects. The PNECs and AAEQ values for the mixture of both terbutryn and terbutryn-sulfoxide may be lower or equivalent to those of terbutryn alone.

The predicted biocide storage capacity of topsoil (0–30 cm) varied across district compartments, including ground-facade interfaces, areas between these interfaces and SSM systems, and under SSM systems, such as trench and pond. After one-year equivalent rainfall (Fig. S14a), 98 % of the terbutryn and its TPs that directly infiltrated at the ground-facade interface leached from the topsoil, potentially reaching the groundwater (Fig. 5). In comparison, after ten years of equivalent rainfall (2014–2024), 80 % of terbutryn and its TPs leached from topsoil

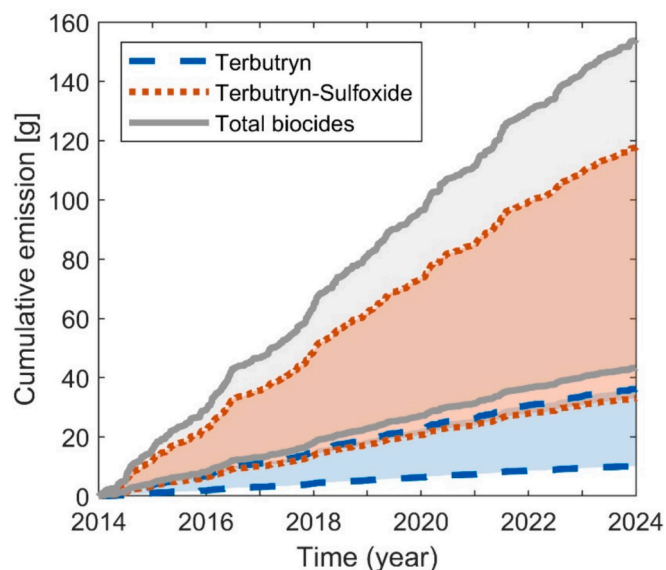


Fig. 3. Cumulative emissions of terbutryn, terbutryn-sulfoxide, and total biocide (terbutryn + terbutryn-sulfoxide) from 2014 to 2024 in the Adelshofen district (Schiltigheim, France), along with associated uncertainties (blue, red, and grey shaded areas), considering low and high initial terbutryn concentrations (C₀) in paints.

following diffuse infiltration from ground-facade interfaces to the SSM systems (Fig. S14b), while 87 % leached beneath SSM systems (Fig. S14c).

Considering uncertainty propagation for the range of C₀ and diffuse runoff coefficients (Table S4), terbutryn contributed only 10 % to 24 % of the total (terbutryn + TPs) mass in topsoil across the district. In contrast, terbutryn-sulfoxide constituted 32 % to 76 %, while unknown secondary TPs represented 1 % to 58 % of the total (terbutryn + TPs) mass in soil (Fig. 5 and Table S4). Secondary TPs were predominant in topsoil directly collecting facade runoff, whereas higher organic carbon content likely enhanced sorption and limited the degradation of terbutryn-sulfoxide in the SSM systems (Fig. 5 and Table S4).

3.4. Emission and transport of terbutryn and TPs under painting scenarios

In scenario P1, where buildings were repainted in 2024 with paints containing the same concentration of terbutryn as in 2014 and considering high C₀, the mass of terbutryn and terbutryn-sulfoxide in the topsoil increased until August 2031 and then gradually declined (Fig. 6a). By 2045, the amount of terbutryn and terbutryn-sulfoxide in soil (5.4 g) corresponded to 83 % of the maximum concentrations in 2031 (6.6 g) (Fig. 6a). In scenario P2, where a paint without biocides was used in 2024, the mass of terbutryn and terbutryn-sulfoxide in the soil decreased from 2024 onwards, with 30 % of the initial mass remaining until 2030. By 2038, the biocide masses in the soil returned to 10 % of the maximum stored in 2024 (Fig. 6b). These findings highlight the importance of implementing measures to prevent the release of urban biocides in order to reduce mass flux towards groundwater. Even in scenario P2, where no new biocides are emitted, the soil can continue to serve as a source of biocide leaching into groundwater.

Overall, these results underscore that, even with a transition to biocide-free facade coatings, residues of terbutryn and terbutryn-sulfoxide may persist in soil for decades, with primary dissipation via biocide leaching rather than degradation. This poses risks to groundwater and drinking water. Although our study is limited to the top 30 cm, the results indicate significant infiltration towards groundwater. This is further supported by recent detections of various urban biocides, including terbutryn and its transformation products, in urban groundwater systems (Hensen et al., 2018; Pinasseau et al., 2020). Furthermore, our assessment of biocide degradation only considered terbutryn-sulfoxide, while the fate of secondary TPs, such as terbutryn-2-hydroxy and terbutryn-desethyl-2-hydroxy (Bollmann et al., 2017a; Junginger et al., 2022), remains unknown. Additionally, the effects on non-target organisms in soils and groundwater remain uncertain, since comprehensive data on the sorption, leaching, degradability, and ecotoxicological effects of terbutryn TPs in deeper soil layers are currently lacking.

4. Conclusions

Biocides, such as terbutryn, are continuously released from building facades during rainfall events, leading to chronic contamination of runoff and soil in urban districts. Our study underscores the importance of combining field investigations with modeling to quantify the emissions, accumulation, and degradation of urban biocides and their transformation products (TPs) at the district scale. Field investigations revealed widespread contamination by terbutryn and its TPs in water, soil, sediment, and vegetation within the district, which may affect freshwater ecosystems even ten years after the district construction.

The developed model suggested that terbutryn contamination could persist in topsoil for up to two decades after emissions from facades cease. While our study advanced the understanding of the emission and transport of terbutryn and its main TP (terbutryn-sulfoxide) in urban districts, the combined effects of terbutryn-sulfoxide with terbutryn and other TPs remain unknown. The long-term ecotoxicological effects in soil, sediment, and urban water require further investigation,

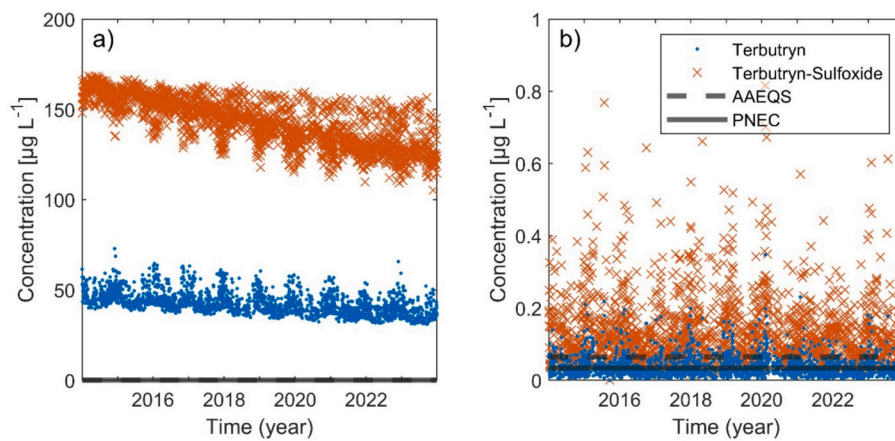


Fig. 4. Concentrations of terbutryn and its transformation product terbutryn-sulfoxide (a) in runoff at the ground-facade interfaces, and (b) in runoff flowing into the trench and pond, over the 10 years following paint application (2014–2024), considering the high initial terbutryn concentrations in paint (C_0). Full black lines indicate the PNEC value ($0.034 \mu\text{g L}^{-1}$), while dashed black lines represent the AAEQS value ($0.065 \mu\text{g L}^{-1}$).

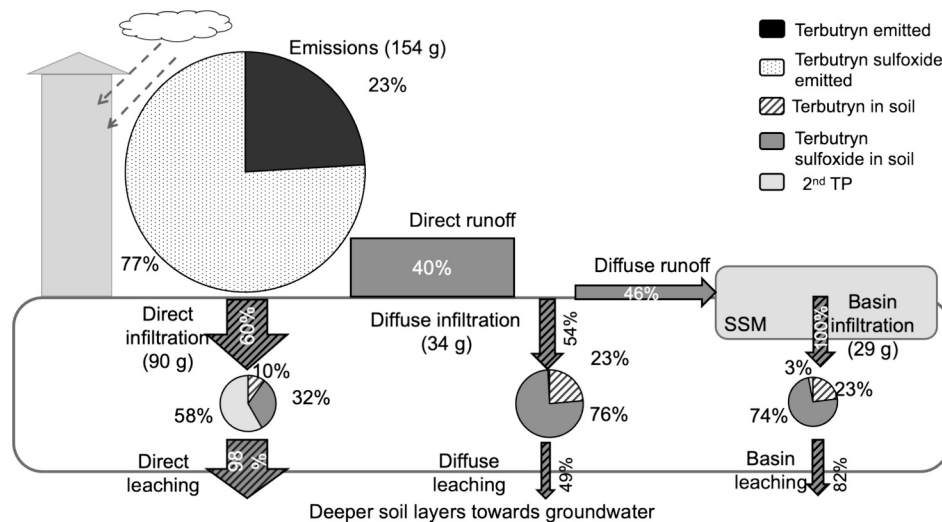


Fig. 5. Mass balance of terbutryn and its transformation products (TPs) in the district topsoil (0–30 cm) over a ten-year period (2014–2024) following initial painting. The balance incorporates direct runoff at the ground-facade interfaces, including direct infiltration and leaching into deeper soil layers, as well as biocide runoff towards the SSM system, involving diffuse infiltration and leaching into deeper layers. The pie charts depict the proportions of terbutryn, terbutryn-sulfoxide, and secondary TPs in topsoil following infiltration. The sizes of the pie charts and arrows are proportional to the biocide masses and fluxes. The mass balance corresponds to high (82 mg m^{-2}) initial concentrations (C_0) of terbutryn in paints, with mean runoff coefficients observed during the 2021 sampling campaign (Fig. S10: 55 % for the pond sub-catchment and 36 % for the trench sub-catchment).

particularly considering biocide TPs. Our results emphasize the crucial role of data availability to establish accurate biocide mass balances at the district scale and identify entry points for biocides into the subsurface. This requires systematic characterization of facades and surface areas within the district, as well as high-quality monitoring data, including water runoff and biocide concentrations. The modeling framework enabled to identify prevailing biocide mass transport, including surface transport by runoff and reactive transport through topsoil to deeper soil layers and groundwater. This framework paved the way for assessing biocide emission, transport, and persistence in ungauged districts where scenarios and hypotheses must compensate for data gaps. Predicted reactive transport of terbutryn and its TPs through soil was significantly affected by soil properties and degradation rates. Our approach primarily focused on topsoil reactivity (0–30 cm). Hence, future studies may consider multi-soil layer models with specific reactivity to assess biocide transport to groundwater.

Regarding Sustainable Stormwater Management (SSM), our results indicate that biocide infiltration into subsurface and groundwater predominantly occurs near facades before reaching SSM systems.

Groundwater protection strategies may involve replacing gravel splash strips around facades with organic-rich materials, such as wood chips, or incorporating activated carbon filters, albeit at a significant cost. Additionally, vegetated infiltration systems in SSM may serve as sinks for biocides, enhancing their retention, degradation and vegetation uptake.

CRediT authorship contribution statement

Laura Sereni: Writing – original draft, Visualization, Validation, Software, Formal analysis, Data curation, Conceptualization. **Tobias Junginger:** Writing – original draft, Visualization, Validation, Software, Methodology, Investigation, Formal analysis, Data curation, Conceptualization. **Sylvain Payraudeau:** Writing – review & editing, Validation, Supervision, Software, Resources, Project administration, Methodology, Conceptualization. **Gwenael Imfeld:** Writing – review & editing, Validation, Supervision, Software, Resources, Project administration, Methodology, Funding acquisition, Formal analysis, Conceptualization.

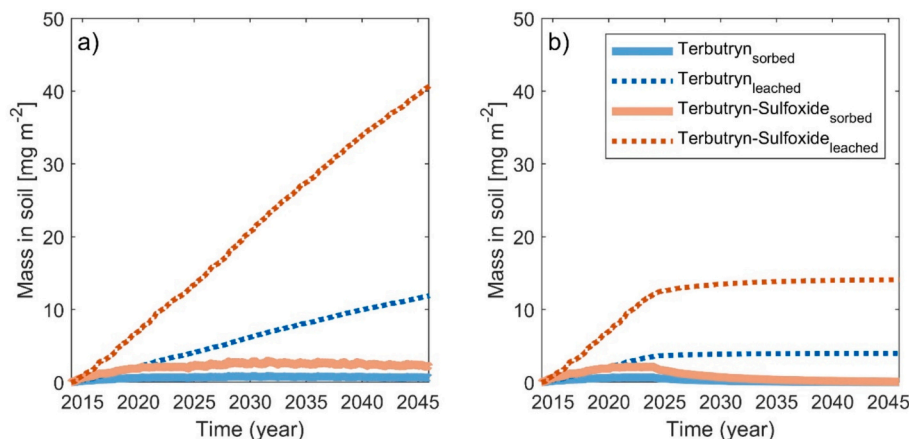


Fig. 6. Normalized masses of terbutryn (blue) and terbutryn-sulfoxide (orange) in soil (sorbed) and leached towards groundwater over a 30-year period (2014–2045) for scenarios P1 (a), i.e., facade repainting 2024 with paints containing the same concentration of terbutryn as in 2014, and P2 (b), i.e., facade repainting 2024 with biocide-free paints.

Declaration of competing interest

The authors declare that they have no known competing financial interests or personal relationships that could have appeared to influence the work reported in this paper.

Data availability

Data will be made available on request.

Acknowledgements

This research received funding from the European Union under the European Regional Development Fund (ERDF) through the INTERREG V and VI support measures in the Upper Rhine, as part of the NAVEBGO project 5.3, which focuses on the sustainable reduction of biocide inputs into groundwater in the Upper Rhine region, and through the ReactiveCity project A3-4. LIDAR and rainfall data were generously provided by the Eurométropole de Strasbourg (EMS). The authors would like to thank the City of Schiltigheim for logistical support and facilitating the field experiment, and express their gratitude to Delphine Thallinger, Benoît Guyot, and Eric Pernin for their contributions to experiment preparation and fieldwork, as well as to Felicia Linke for valuable discussions. Concentration measurements were conducted at the PACITE platform of the University of Strasbourg at ITES (Strasbourg, France).

Appendix A. Supplementary data

Supplementary data to this article can be found online at <https://doi.org/10.1016/j.scitotenv.2024.176269>.

References

- Barbosa, A.E., Fernandes, J.N., David, L.M., 2012. Key issues for sustainable urban stormwater management. *Water Res.* 46, 6787–6798. <https://doi.org/10.1016/j.watres.2012.05.029>.
- Bester, K., Vollertsen, J., Bollmann, U.E., 2014. Water Driven Leaching of Biocides From Paints and Renders (Methods for the Improvement of Emission Scenarios Concerning Biocides in Buildings No. Pesticide Research No. 156, 2014).
- Bollmann, U.E., Tang, C., Eriksson, E., Jo, K., Vollertsen, J., Bester, K., 2014. Biocides in urban wastewater treatment plant influent at dry and wet weather: concentrations, mass flows and possible sources. *Water Res.* <https://doi.org/10.1016/j.watres.2014.04.014>.
- Bollmann, U.E., Minelgaite, G., Schlüsener, M., Ternes, T., Vollertsen, J., Bester, K., 2016. Leaching of terbutryn and its photodegradation products from artificial walls under natural weather conditions. *Environ. Sci. Technol.* 50, 4289–4295. <https://doi.org/10.1021/acs.est.5b05825>.
- Bollmann, U.E., Fernández-Calviño, D., Brandt, K.K., Storgaard, M.S., Sanderson, H., Bester, K., 2017a. Biocide runoff from building facades: degradation kinetics in soil. *Environ. Sci. Technol.* 51, 3694–3702. <https://doi.org/10.1021/acs.est.6b05512>.
- Bollmann, U.E., Minelgaite, G., Schlüsener, M., Ternes, T.A., Vollertsen, J., Bester, K., 2017b. Photodegradation of octylisothiazolinone and semi-field emissions from facade coatings. *Sci. Rep.* 7, 41501. <https://doi.org/10.1038/srep41501>.
- Bork, M., Lange, J., Graf-Rosenfellner, M., Hensen, B., Olsson, O., Hartung, T., Fernández-Pascual, E., Lang, F., 2021. Urban storm water infiltration systems are not reliable sinks for biocides: evidence from column experiments. *Sci. Rep.* 11, 7242. <https://doi.org/10.1038/s41598-021-86387-9>.
- Bork, M., Engel, Johannes, Krämer, Alexander, Lange, Jens, 2022. FReWaB-PLUS (Freiburger Regenwasserbewirtschaftung plus Stofftransport) [WWW Document]. FReWaB-PLUS: Mobilisierung von Bioziden in Stadtgebieten. URL: <https://www.biozidauswaschung.de> (accessed 10.1.22).
- Burkhardt, M., Junghans, M., Zuleeg, S., Boller, M., Schoknecht, U., Lamani, X., Bester, K., Vonbank, R., Simmler, H., 2009. Biozide in Gebäudewänden – ökotoxikologische Effekte, Auswaschung und Belastungsabschätzung für Gewässer. *Environ. Sci. Eur.* 21, 36–47. <https://doi.org/10.1007/s12302-008-0033-1>.
- Burkhardt, M., Zuleeg, S., Vonbank, R., Schmid, P., Hean, S., Lamani, X., Bester, K., Boller, M., 2011. Leaching of additives from construction materials to urban storm water runoff. *Water Sci. Technol.* 63, 1974–1982. <https://doi.org/10.2166/wst.2011.128>.
- Burkhardt, M., Engelke, D., Gehrig, S., Hochstrasser, F., Rohr, M., Tietje, O., 2020. COMLEAM - Manual Version 3.0.
- Coutu, S., Del Giudice, D., Rossi, L., Barry, D.A., 2012a. Modeling of facade leaching in urban catchments. *Water Resour. Res.* 48. <https://doi.org/10.1029/2012WR012359>.
- Coutu, S., Rota, C., Rossi, L., Barry, D.A., 2012b. Modelling city-scale facade leaching of biocide by rainfall. *Water Res.* 46, 3525–3534. <https://doi.org/10.1016/j.watres.2012.03.064>.
- Duque, L.F., 2020. IETD: Inter-event Time Definition.
- European Commission, 2011. Terbutryn EQS Dossier.
- European Commission, 2022. JRC Photovoltaic Geographical Information System (PVGIS) - European Commission [WWW Document]. URL: https://re.jrc.ec.europa.eu/pvg_tools/en/ (accessed 2.8.23).
- Fernández-Calviño, D., Rousk, J., Bååth, E., Bollmann, U.E., Bester, K., Brandt, K.K., 2021. Short-term toxicity assessment of a triazine herbicide (terbutryn) underestimates the sensitivity of soil microorganisms. *Soil Biol. Biochem.* 154, 108130. <https://doi.org/10.1016/j.soilbio.2021.108130>.
- Finizio, A., Guardo, A.D., Arnoldi, A., Vighi, M., Fanelli, R., 1991. Different approaches for the evaluation of Kow for s-triazine herbicides. *Chemosphere* 23, 801–812. [https://doi.org/10.1016/0045-6535\(91\)90084-Q](https://doi.org/10.1016/0045-6535(91)90084-Q).
- Finizio, A., Vighi, M., Sandroni, D., 1997. Determination of n-octanol/water partition coefficient (Kow) of pesticide critical review and comparison of methods. *Chemosphere* 34, 131–161. [https://doi.org/10.1016/S0045-6535\(96\)00355-4](https://doi.org/10.1016/S0045-6535(96)00355-4).
- Gao, J., Garrison, A.W., Hoehamer, C., Mazur, C.S., Wolfe, N.L., 2000. Uptake and phytotransformation of organophosphorus pesticides by axenically cultivated aquatic plants. *J. Agric. Food Chem.* 48, 6114–6120. <https://doi.org/10.1021/jf9904968>.
- Gilevska, T., Wiegert, C., Droz, B., Junginger, T., Prieto-Espinoza, M., Borreca, A., Imfeld, G., 2022. Simple extraction methods for pesticide compound-specific isotope analysis from environmental samples. *MethodsX*, 101880. <https://doi.org/10.1016/j.mex.2022.101880>.
- Goulden, S., Portman, M.E., Carmon, N., Alon-Mozes, T., 2018. From conventional drainage to sustainable stormwater management: beyond the technical challenges. *J. Environ. Manag.* 219, 37–45. <https://doi.org/10.1016/j.jenvman.2018.04.066>.
- Hensen, B., Lange, J., Jackisch, N., Zieger, F., Olsson, O., Kümmerer, K., 2018. Entry of biocides and their transformation products into groundwater via urban stormwater

- infiltration systems. *Water Res.* 144, 413–423. <https://doi.org/10.1016/j.watres.2018.07.046>.
- Junginger, T., 2023. *Transport and Degradation of Urban Biocides From Facades to Groundwater* (PhD Thesis). Université de Strasbourg.
- Junginger, T., Payraudeau, S., Imfeld, G., 2022. Transformation and stable isotope fractionation of the urban biocide terbutryn during biodegradation, photodegradation and abiotic hydrolysis. *Chemosphere* 305, 135329. <https://doi.org/10.1016/j.chemosphere.2022.135329>.
- Junginger, T., Payraudeau, S., Imfeld, G., 2023. Emissions of the urban biocide terbutryn from facades: the contribution of transformation products. *Environ. Sci. Technol.* <https://doi.org/10.1021/acs.est.2c08192>.
- Kresmann, S., Arokia, A.H.R., Koch, C., Sures, B., 2018. Ecotoxicological potential of the biocides terbutryn, octhiline and methylisothiazolinone: underestimated risk from biocidal pathways? *Sci. Total Environ.* 625, 900–908. <https://doi.org/10.1016/j.scitotenv.2017.12.280>.
- Linke, F., Olsson, O., Preusser, F., Kümmerer, K., Schnarr, L., Bork, M., Lange, J., 2021. Sources and pathways of biocides and their transformation products in urban storm water infrastructure of a 2 ha urban district. *Hydrol. Earth Syst. Sci.* 25, 4495–4512. <https://doi.org/10.5194/hess-25-4495-2021>.
- Linke, F., Edun, O., Junginger, T., Payraudeau, S., Preusser, F., Imfeld, G., Lange, J., 2023. Biocides in soils of urban stormwater infiltration systems—indications of inputs from point and non-point sources. *Water Air Soil Pollut.* 234, 586. <https://doi.org/10.1007/s11270-023-06613-0>.
- Luft, A., Wagner, M., Ternes, T.A., 2014. Transformation of biocides irgarol and terbutryn in the biological wastewater treatment. *Environ. Sci. Technol.* 48, 244–254. <https://doi.org/10.1021/es403531d>.
- Muerdter, C.P., Powers, M.M., Chowdhury, S., Mianeki, A.L., LeFevre, G.H., 2022. Rapid plant uptake of isothiazolinone biocides and formation of metabolites by hydroponic *Arabidopsis*. *Environ Sci Process Impacts* 24, 1735–1747. <https://doi.org/10.1039/D2EM00178K>.
- Paijens, C., Bressy, A., Frère, B., Tedoldi, D., Mailler, R., Rocher, V., Neveu, P., Moilleron, R., 2021. Urban pathways of biocides towards surface waters during dry and wet weathers: assessment at the Paris conurbation scale. *J. Hazard. Mater.* 402, 123765. <https://doi.org/10.1016/j.jhazmat.2020.123765>.
- Pinasseau, L., Wiest, L., Volatier, L., Mermillod-Blondin, F., Vulliet, E., 2020. Emerging polar pollutants in groundwater: potential impact of urban stormwater infiltration practices. *Environ. Pollut.* 266, 115387. <https://doi.org/10.1016/j.envpol.2020.115387>.
- Quednow, K., Püttmann, W., 2007. Monitoring terbutryn pollution in small rivers of Hesse, Germany. *J. Environ. Monit.* 9, 1337–1343. <https://doi.org/10.1039/B711854F>.
- Reiß, F., Kiefer, N., Noll, M., Kalkhof, S., 2021. Application, release, ecotoxicological assessment of biocide in building materials and its soil microbial response. *Ecotoxicol. Environ. Saf.* 224, 112707. <https://doi.org/10.1016/j.ecoenv.2021.112707>.
- Reiß, F., Kiefer, N., Purahong, W., Borcken, W., Kalkhof, S., Noll, M., 2024. Active soil microbial composition and proliferation are directly affected by the presence of biocides from building materials. *Sci. Total Environ.* 912, 168689. <https://doi.org/10.1016/j.scitotenv.2023.168689>.
- Schoknecht, U., Mathies, H., Wegner, R., 2016. Biocide leaching during field experiments on treated articles. *Environ. Sci. Eur.* 28, 6. <https://doi.org/10.1186/s12302-016-0074-9>.
- Turgut, C., 2005. Uptake and modeling of pesticides by roots and shoots of parrotfeather (*Myriophyllum aquaticum*) (5 pp). *Environ. Sci. Pollut. Res. Int.* 12, 342–346. <https://doi.org/10.1065/espr2005.05.256>.
- Vega-García, P., Schwerd, R., Scherer, C., Schwitalla, C., Johann, S., Rommel, S.H., Helmreich, B., 2020. Influence of façade orientation on the leaching of biocides from building façades covered with mortars and plasters. *Sci. Total Environ.* 734, 139465. <https://doi.org/10.1016/j.scitotenv.2020.139465>.
- Vijayaraghavan, K., Biswal, B.K., Adam, M.G., Soh, S.H., Tsen-Tieng, D.L., Davis, A.P., Chew, S.H., Tan, P.Y., Babovic, V., Balasubramanian, R., 2021. Bioretention systems for stormwater management: recent advances and future prospects. *J. Environ. Manag.* 292, 112766. <https://doi.org/10.1016/j.jenvman.2021.112766>.
- Whitehouse, P., Brown, B., Wilkinson, H., Payá Pérez, A., Zaldivar-Comenges, J., Daginnus, K., Deviller, G., Clausen, H., Lofstedt, M., Babut, M., van Vlaardingen, P., Moermond, C., Janssen, M., Ten Hulscher, D., Delbeke, K., Assche, F., Schwaiger, K., Rödinger, W., Geyt, A., Castro-Jiménez, J., 2011. Guidance Document No. 27. Technical Guidance For Deriving Environmental Quality Standards. <https://doi.org/10.2779/43816>.
- Wicke, D., Tatis-Muvdi, R., Rouault, P., Zerball-van Baar, P., Dünnbier, U., Rohr, M., Burkhardt, M., 2022. Emissions from building materials—a threat to the environment? *Water* 14, 303. <https://doi.org/10.3390/w14030303>.
- Wittmer, I.K., Bader, H.-P., Scheidegger, R., Singer, H., Lück, A., Hanke, I., Carlsson, C., Stamm, C., 2010. Significance of urban and agricultural land use for biocide and pesticide dynamics in surface waters. *Water Res.* 44, 2850–2862. <https://doi.org/10.1016/j.watres.2010.01.030>.
- Wittmer, I.K., Scheidegger, R., Stamm, C., Gujer, W., Bader, H.-P., 2011. Modelling biocide leaching from facades. *Water Res.* 45, 3453–3460. <https://doi.org/10.1016/j.watres.2011.04.003>.